Computational Modeling of Nanoparticle Heating for Treatment Planning of Plasmonic Photothermal Therapy in Pancreatic Cancer

Santiago Manrique-Bedoya[1*], Chris Moreau[3], Sandeep Patel[3], Yusheng Feng[1], Kathryn Mayer[2]

[1] Department of Mechanical Engineering at The University of Texas at San Antonio, TX, USA
[2] Department of Physics and Astronomy at The University of Texas at San Antonio, TX, USA
[3] Transplant Center at UT Health San Antonio, TX, USA
*santiago.manriquebedoya@utsa.edu

Abstract

Pancreatic cancer is one of the deadliest cancers with a 7% survival rate at five years from diagnosis. The limited number of treatment options for patients who are diagnosed with late-stage disease is a major contributor to this problem. Therapeutic modalities such as radiofrequency ablation (RFA) and laser interstitial thermal therapy (LITT) have emerged as potential tumor debulking tools. However, the outcome of these tissue treatments *in-vivo* is difficult to predict due to visualization constraints, causing a reduction in specificity and increasing pancreatitis risk. Gold nanoparticles (GNPs) may improve the efficacy of thermal therapy. Before *in-vivo* studies are undertaken, we propose a computational model of plasmonic photothermal therapy (PPTT) to study the laser-particle-tissue interactions and determine the optimum parameters for this treatment. This model may also serve as a future treatment planning tool for physicians.

Key words: Photothermal heating, plasmonic heating, gold nanoparticles, plasmonic photothermal therapy, laser thermal effect

1. Introduction

In recent years, new techniques have been developed as alternatives for tumor treatment, some of these techniques focus on enabling hyperthermia which is defined as heating tissue to a temperature between 41 and 47°C for at least 20-30 minutes [1, 2], thus causing severe damage to the tumorous tissue due to its reduced heat tolerance, but also damaging the healthy tissue in the process.

The more successful alternatives have been those that use light to induce tissue hyperthermia (e.g. LITT and PDT). More recently, therapeutic approaches that operate in the near infrared (NIR) region, such as photothermal therapy (PTT) have shown more promise due to the high physiological transmissivity observed in this range, which allows minimizing undesired tissue absorption and subsequent heating [3].

PTT uses agents that absorb light and thus induce electronic excitation that leads to overheating of the surrounding media. PTT agents include natural tissue chromophores and dye molecules; moreover, research and advances in nanotechnology have provided a new PTT agent: metallic nanoparticles, more specifically, gold nanoparticles (GNPs). With a better understanding of the mechanisms by which GNPs can absorb light and transform it into heat [4], new approaches to photothermal therapy are being developed, such as the use of near infrared lasers that minimize healthy tissue heating while exciting the nanoparticles so that the heating is localized in the tumor region. This new therapeutic approach is called plasmonic photothermal therapy (PPTT).

In this paper we aim to develop a computational model to study the optical properties of gold nanoparticles, the plasmonic heating, and the heat transfer effect in the surrounding media so that parameters crucial to the development of *in-vivo* experiments can be optimized.

2. Methods

We compared different shapes of nanoparticles (nanorod, nanosphere, nanobipyramid) and studied the temperature gradient induced in the surrounding media in both water and tissue. The particles were modeled using SOLIDWORKS® CAD software and imported into COMSOL Multiphysics® via LiveLink™. Tissue properties were extracted from literature [5, 6]. The photothermal behavior of the GNPs when illuminated by a 20 mW, 808 nm laser was described by: (1) using the RF Module to find the amount of energy absorbed, and (2) using the Coefficient Form PDE module to solve the heat equation using the previously calculated energy absorbed as the heat source. This setup allowed the calculation of temperature gradient surrounding each particle.

2.1 RF Module

By exposing GNPs to light at their resonance wavelength, the metallic nanoparticles experience a synchronized oscillation, generated by the conduction-band electrons, that terminates in either light scattering or absorption [2, 4]. This oscillation is called localized surface plasmon resonance (LSPR) and can be described using Maxwell's equations.
The optical properties of the GNPs were studied using the RF Module in COMSOL 5.3®. In this module, Maxwell's equations are represented as the wave equation for electric field

$$\nabla \times \mu_r^{-1}(\nabla \times E) - k_0^2 \varepsilon E = 0$$

Where μ_r is the relative permeability of the particle, $\boldsymbol{E}$ is the electric field, $\boldsymbol{k}_0$ is the wave propagation vector, and ε is the dielectric permittivity of gold which contains both the real and imaginary portions.
When solving for the scattered field, the background electric field, or incident light, for a plane wave polarized along the x-axis and propagating along the z-axis is defined as

$$E_b = E_0 e^{\left(-j\frac{2\pi n}{\lambda}z\right)}\hat{\imath}$$

With $\boldsymbol{E}_0$ being the amplitude of the wave (V/m), n the refractive index of the medium, and λ the wavelength (nm).

The optical properties of the different types of particles were analyzed under plane waves with different wavelengths using the parametric sweep and the frequency domain study. The dielectric permittivity of gold was extracted from literature [7]. To truncate the computational domain without introducing significant artifacts to the solution, a perfectly matched layer (PML) of $\lambda/2$ is set around the nanoparticle of interest as shown in Figure 1 [8].

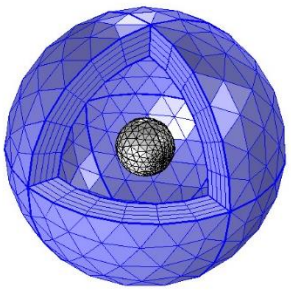

Figure 1. PML around a nanosphere for domain truncation in RF module computations

The mesh applied to the system was physics-controlled with a *finer* size.

2.2 PDE Module

The effect of heat transfer in different media will be assessed using the Coefficient Form PDE module. Initially, a stationary study is set, and the general formula is reduced to the heat equation

$$\nabla \cdot (-k\nabla T) = f$$

Where k is the thermal conductivity of the surrounding medium (e.g. water) and f is the energy absorbed by the GNPs which is then transformed and released as heat.

The PML is no longer needed so the surrounding media is initially formed by a $3\mu m$ sphere of water. The initial temperature is set at 37°C and a Dirichlet boundary condition of 37°C is set to the outermost boundaries of the system as shown in Figure 2

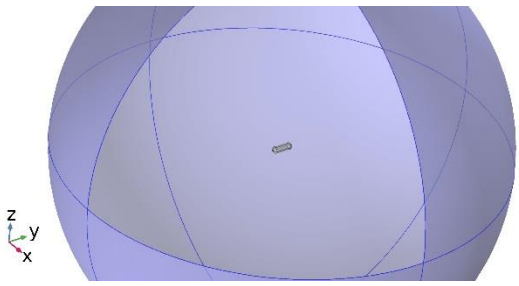

Figure 2. Water sphere of $\boldsymbol{3\mu m}$ around a nanorod for computational measurement of heat distribution around the nanoparticle

3. Results & Discussion

The different shapes and sizes of nanoparticles were assessed for NIR implementation by calculating the absorbance cross section over a wide range of wavelengths. This cross section can be calculated as the ratio of energy absorbed to incident irradiance

$$\sigma_{abs} = \frac{W_{abs}}{S_{in}}$$

With W_{abs} being the energy absorbed and S_{in} the incident irradiance, also known as Poynting vector. The energy absorbed by the nanoparticles is readily

calculated in COMSOL by integrating the power dissipation energy over the volume of the nanoparticle

$$W_{abs} = \iiint_{\Omega} Q_h \, d\Omega$$

Q_h is COMSOL's predefined variable for power dissipation energy and given its dependency on wavelength (λ), a parametric sweep over varying values of λ was placed to calculate the optical cross section spectra. An example of the absorbance cross section calculated over a range of wavelengths is shown in Figure 3.

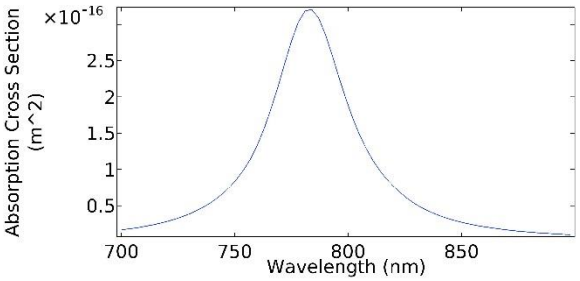

Figure 3. Absorption cross section of a gold nanorod with 60 nm length and aspect ratio of 3.3

The particles exhibit a LSPR peak within the therapeutic window (700 nm – 1000 nm), except the nanospheres which showed a peak in the visible range (400 nm – 700 nm). The resonance wavelength for each specimen is recorded in Table 1 below

Table 1. LSPR for the different types of nanoparticles

Nanoparticle Type	Dimensions (nm)	LSPR Peak (nm)
Nanorod	80	804
Nanorod	60	784
Nanobipyramid	110	783
Nanobipyramid	146	820
Nanosphere	40	526
Nanosphere	150	650

The dimensions recorded in Table 1 are the length in the case of the rods and bipyramids and the diameter for the spheres. In the case of the nanorods, the aspect ratio was 3.3 for both, whereas the bipyramids had different dimensions overall: the longer bipyramid had a 55 nm width and 8 nm tip radius; the shorter bipyramid had a 40 nm width and a 6.2 nm tip radius. It can be noted that both the rods and the bipyramids are well suited for NIR applications and that spheres are better fit for use under visible light illumination. The energy absorbed by the different NPs when illuminated by a 20 mW NIR laser (808 nm) is recorded in Table 2.

Table 2. Energy absorbed by the nanoparticles

Nanoparticle Type	Dimensions (nm)	Energy Absorbed (W/m^3)
Nanorod	80	1.37E18
Nanorod	60	7.41E17
Nanobipyramid	110	4.90E17
Nanobipyramid	146	4.40E17
Nanosphere	40	5.81E14
Nanosphere	150	8.43E14

The size of the particle is significantly smaller in comparison to the size of the incident beam thus a plane wave assumption is in place. Note that the values reported in Table 2 were measured with a wave propagating along the z-axis and polarized along the y-axis as shown in Figure 4.

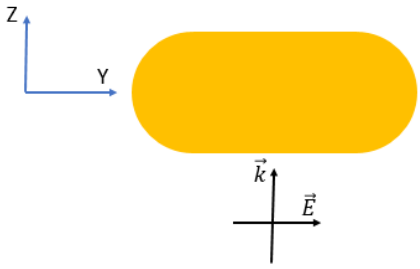

Figure 4. Schematic depicting the nanoparticle location in the YZ-plane with its longitudinal axis oriented along the Y-axis, and the propagating plane wave along Z-axis and polarized along the Y-axis.

It can be noted that the larger gold nanorod absorbs the highest amount of energy due to its resonance wavelength being the closest to the wavelength of the laser. However, the energy absorbed is highly dependent on the orientation of the nanoparticle with respect to the incident light; therefore, an average energy absorbed is calculated by rotating the particle between 0° (longitudinal axis along Y) and 90° (longitudinal axis along Z).

Due to symmetry, the change in light orientation did not affect the amount of energy absorbed by the nanospheres (NS). This energy is then used as the source in the PDE Module (see section 2.2) to obtain the temperature increase due to the energy absorbed by each particle. The average energy absorbed by the nanorods (NR) and bipyramids (BP), along with the respective maximum temperature reached in a single particle is reported in Table 3.

Table 3. Average energy and maximum temperature reached by a single gold nanoparticle

Nanoparticle Type	Average Energy Absorbed (W/m^3)	Max Temperature (°C)
NR (80 nm)	6.81E17	252
NR (60 nm)	3.71E17	93.9
BP (110 nm)	2.45E17	136
BP (146 nm)	2.20E17	203
NS (40 nm)	5.81E14	37.2
NS (150 nm)	8.43E14	40.6

The 80 nm nanorod shows the higher energy absorbed and thus the higher temperature increase and is therefore selected as the best suited shape to enhance the photothermal effect for treating tumorous tissue.

The next step is to evaluate the cluster effect. For this purpose, we have arranged a cluster of nanorods following a cubic array and each NR has been given the same energy as NR 80 reported in Table 3. The spacing between each nanoparticle was calculated according to a concentration of 22 nM and the isothermal curves in Figure 5 show that the hyperthermic effect (tissue reaching a temperature of at least 43°C) with this cluster of 423 nm^3 reaches well beyond 1 µm giving us a good prospect of the efficacy of this approach.

Given the size difference between the nanoparticle (nm – µm) and the tissue (cm), it is safe to assume the nanoparticle clusters can be included in the tissue-level simulations as point sources. In these simulations, pancreatic tissue is represented by a cylindrical phantom with a concentric cylindrical fiber tip for laser light delivery and two point sources to study the effect of distance from the light source and heat generated as shown in Figure 6. The point sources are located at 3 mm and 7 mm from the fiber tip.

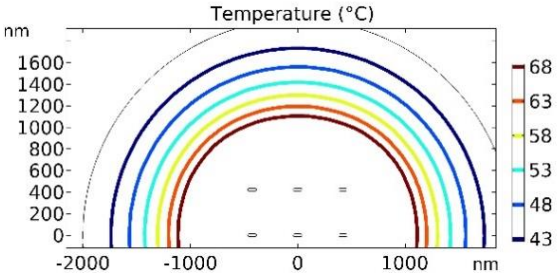

Figure 5. Effect of a cluster of nanorods at 22 nM.

In this preliminary study, the effect of distance from the light source on heat generation was manually implemented and the tissue properties were those reported for pancreas under laser illumination outside of the therapeutic window (1064 nm) [6]. Figure 7 illustrates the effects of a 20 mW laser in the NIR (808 nm) and the point sources simulate clusters of 1000 GNRs each. The mathematical formalism used for the laser-tissue interaction is described elsewhere [6] and implemented following the general heat equation.

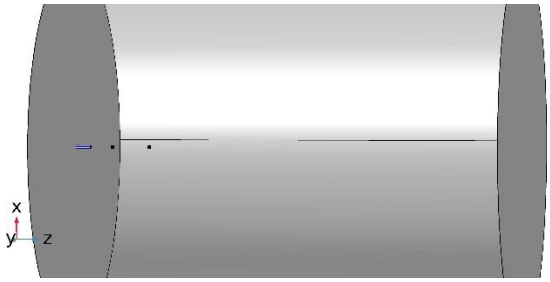

Figure 6. Tissue model showing the cylindrical tissue phantom, the fiber tip and the point sources at different distances from the fiber.

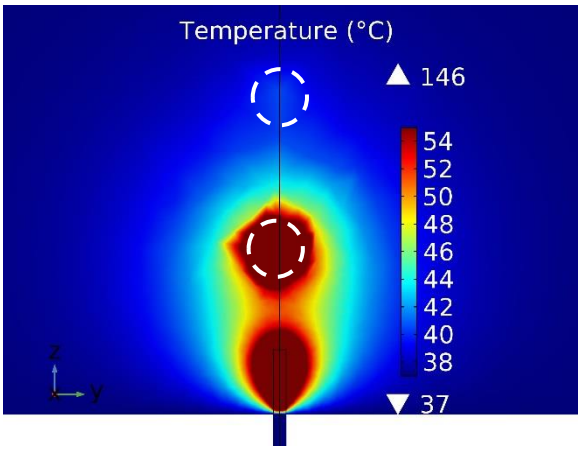

Figure 7. Effect of nanoparticle clusters at different distances (3 mm and 7 mm) from the fiber tip.

Perfusion of the blood is not considered in this model and the initial temperature is set to 37ºC everywhere. It is shown that the tissue around the fiber tip and the first cluster reaches hyperthermia in a region of 2 mm around these sources, and that the second cluster induces hyperthermia in a smaller region (<1mm). However, the effect around the fiber tip can be associated to the implementation of tissue properties outside of the therapeutic window since the tissue absorptivity is highly dependent on the wavelength.

4. Conclusion

The models developed herein successfully describe the mechanisms of light absorption by the nanoparticles, the subsequent nanoparticle heating and the resulting heat transfer in the surrounding medium. Additionally, the proper implementation of NP clusters showed to be crucial for effective results.

The accuracy of the computational model can provide insight, and aid in the design of *in-vivo* experiments based on the simulations' results. The effect around the laser tip can be minimized using tissue properties measured using a wavelength within the therapeutic window. Future work will focus on the proper implementation of the tissue properties, further refinement of the model so that more realistic laser irradiance is included, and a more comprehensive mathematical model that encompasses light diffusion in tissue as well as the heat transfer.

References

1. Svaasand, L.O., C.J. Gomer, and E.J.L.i.M.S. Morinelli, *On the physical rationale of laser induced hyperthermia.* 1990. **5**(2): p. 121-128.
2. Huang, X., et al., *Plasmonic photothermal therapy (PPTT) using gold nanoparticles.* 2008. **23**(3): p. 217.
3. Bayazitoglu, Y., et al., *An overview of nanoparticle assisted laser therapy.* 2013. **67**: p. 469-486.
4. Kennedy, L.C., et al., *A new era for cancer treatment: gold-nanoparticle-mediated thermal therapies.* 2011. **7**(2): p. 169-183.
5. Jacques, S.L.J.P.i.M. and Biology, *Optical properties of biological tissues: a review.* 2013. **58**(11): p. R37.
6. Saccomandi, P., et al., *Theoretical analysis and experimental evaluation of laser-induced interstitial thermotherapy in ex vivo porcine pancreas.* 2012. **59**(10): p. 2958-2964.
7. Johnson, P.B. and R.-W.J.P.r.B. Christy, *Optical constants of the noble metals.* 1972. **6**(12): p. 4370.
8. Johnson, S.G.J.L.n., Massachusetts Institute of Technology, Massachusetts, *Notes on perfectly matched layers (PMLs).* 2008. **29**.